

PRICING AMERICAN LOOKBACK OPTIONS UNDER A STOCHASTIC VOLATILITY MODEL

DONGHYUN KIM, JUNHUI WOO, AND JI-HUN YOON

ABSTRACT. In this study, we deal with American lookback option prices on dividend-paying assets under a stochastic volatility (SV) model. By using the asymptotic analysis introduced by Fouque et al. [17] and the Laplace-Carson transform (LCT), we derive the explicit formula for the option prices and the free boundary values with a finite expiration whose volatility is driven by a fast mean-reverting Ornstein-Uhlenbeck process. In addition, we examine the numerical implications of the SV on the American lookback option with respect to the model parameters and verify that the obtained explicit analytical option price has been obtained accurately and efficiently in comparison with the price obtained from the Monte-Carlo simulation.

1. Introduction

Even though the Black-Scholes model has been widely used for pricing and hedging financial derivatives because of its theoretical simplicity and practical usefulness, it is well known that the assumption of a standard Black-Scholes model [3] for underlying asset prices do not reflect the empirical evidence in the financial market. Actually, the assumption of the Black-Scholes model is in flat implied volatilities, which is inconsistent with empirical results verifying that the implied volatilities of the equity options display the smile or skew phenomenon. Before the 1987 crash, the curve of implied volatilities against the strike price was occasionally found to have U-shape with minimum at or near the money but, after the crash, the typical geometry of implied volatilities appeared in the form of the smile. Another one among the assumption of the Black-Scholes model is that the stock price has a log-normal distribution. However, in the real market, there are some excess skewness and leptokurtosis as the properties of the risk-neutral probability distribution in contrast to the log-normal distribution. Therefore, reflecting these empirical features in the

Received February 19, 2022; Accepted May 2, 2022.

2020 *Mathematics Subject Classification.* 60H30, 91G15, 91G20.

Key words and phrases. American lookback options, stochastic volatility, Laplace-Carson transform, Monte-Carlo simulation.

The research of J.-H. Yoon was supported by the National Research Foundation of Korea grants funded by the Korean government (NRF-2019R1A2C108931011).

real market, it became necessary to develop another model. Stochastic volatility models have become useful for derivative pricing and hedging for dozens of years since the existence of a nonflat implied volatility surface has been noticed and become more pronounced. In particular, many exogenous variables and extraordinary volatility behaviors have exerted a significant effect on the market after the global financial crisis in 2007-2008, as seen in Choi et al. [6]. Hence, participants in financial transactions have begun to pay attention to the models that can predict the movement of financial assets. So, considering that the volatility of an underlying asset follows an exogenous stochastic process after the financial crisis in 2007-2008, (pure) stochastic volatility SV model are considerably more popular for describing their dynamics and reflecting real situations in financial markets. The Heston model (cf. Heston [20]) and the fast mean-reverting SV model introduced by Fouque et al. [17] have become representative SV models, which are designed to capture the phenomenon of the mean-reversion of volatility in the financial market. Agarwal et al. [2] utilized the maturity randomization method to approximate the American option price under SV models, whose volatility process is characterized by fast- and slow-scale mean-reverting factors, and Zhu and Chen [37] investigated the analytic formulas for perpetual American options under a SV environment with a fast-mean-reverting process.

Lookback options are a type of exotic options with path dependency, where option payoff depends on the maximum or minimum value of the underlying asset during the contract's lifetime. Generally, lookback options are sorted by whether the strike price is a maximum (or minimum) variable process, or a fixed constant for the floating or fixed strike options. In both cases, it is difficult to forecast the pricing of the lookback options as the option price at any time relies on the path from the underlying asset, as well as the underlying asset at that point. There have been many studies on the analytic valuation of lookback options using the Black-Scholes or SV frameworks, or the structures of the model dynamics reflecting some default risks. Most importantly, analytic formulas for floating-strike and fixed-strike lookback options have been introduced by Goldman et al. [19] and Conze and Viswanathan [8] in the Black-Scholes settings. Dai et al. [12] found an explicit closed solution for Quanto lookback options. In addition, Wong and Kwok [34] utilized a new technique for a sub-replicating portfolio and the corresponding replenishing strategy to calculate multistate lookback option values more effectively and easily and demonstrated the relationship between fixed and floating lookback options. Leung [29] used the homotopy analysis technique to obtain an analytical pricing solution for floating-strike and fixed-strike lookback options based on Heston's SV model, and Wong and Chan [33] studied the analytical solutions of lookback options with a multiscale SV model driven by a fast-mean reverting process and a slow-varying volatility process. In addition, Lee [28] examined the approximated solution for the price of the perpetual American lookback option under the SV model and analyzed the effects of SV on option prices in comparison

with those under the classical Black-Scholes model. Moreover, Choi et al. [7] used the Mellin transform and the method using images to derive a closed-form solution to fixed-strike lookback options with default risk as the model settings for default risk.

American option is a financial instrument in which the time to maturity is finite, so that option holders can exercise the option at any time before maturity. In this paper, *we discuss the pricing formula for American-style lookback options with a finite expiration under the SV model driven by the Ornstein-Uhlenbeck process.* The American lookback option is similar to the structure of the American option, but the difference is that the payoff is determined by the maximum (or minimum) value until the time the option is exercised. This article is an extended study of a recent study by Lee [28]. As shown in Lee [28], in the case of the perpetual American option, the time to maturity is infinite. Therefore, the differential equation for the value of the perpetual American option does not include the derivative in terms of time, and the corresponding problems can be much simpler than deriving the pricing formula for the finite expiry American option. To the best of our knowledge, there is no explicit closed-form analytical expression for the formula of the American option or its associated free boundary value, contrary to the perpetual American option.

Therefore, in this study, to find the analytic solutions for the American lookback options, we use the Laplace-Carson transform (LCT). Applying the LCT to PDE problems for the option value, we obtain the closed solutions for the option prices and the optimal boundary values in the transferred frequency domain. Subsequently, by exploiting the inversion of the LCT using the Gaver-Stehfest algorithm, we can find the analytic formulas for the American lookback options using the SV model.

The LCT, a variant of the regular Laplace transform, is an integral transform and has been used in many fields such as physics and railway engineering. LCT is a powerful tool for dealing with dynamical systems formulated by ordinary/partial differential equations (PDEs), simplifying complicated problems. Many studies have addressed financial derivatives on the LCT. Carr [4] introduced the randomization approach that takes into account the LCT of a fixed maturity barrier maximized over barriers. He focused on LCT and its applications to price of an American option with random maturity to obtain semi-explicit solutions for American option prices under the Black-Scholes setting. Kimura [23] derived Russian option prices with finite time horizons using LCT, and Wong and Zhao [35] utilized LCT to investigate the American option prices and its free boundary values under the constant elasticity of variance (CEV) model. In addition, Kimura [26] dealt with the approach of the LCT to option pricing to value defaultable and non-callable convertible bonds (CBs), and Kang et al. [21] found an analytic solution for the price of American strangle options by making use of the LCT. They solved the nonlinear system for the option price using Newton's method, and finally obtained the optimal free boundaries and the values of the options using the techniques of numerical

Laplace inversion. Moreover, Zhou and Wu [36] investigated pricing American Strangles options with constant elasticity volatility (CEV) models using the LCT method.

The main contributions of this paper are as follows: Firstly, the stochastic volatility (SV) models have very complicated model structures compared with the BS model. So, the complex structures of the model dynamics make it very difficult for us to solve the given PDEs. Actually, we cannot solve the PDEs directly. Therefore, to resolve this problem, we use asymptotic analysis on the PDEs to find the analytic solutions for the option prices, where the analytic solutions are given by the sum of the leading order term and the correction order term. Here, to derive the leading order term and the correction order term for the American lookback options, we exploit Laplace-Carson transform (LCT) which is very helpful for us to deal with American option pricing, while Dai and Kwok [10] have just solved the PDEs for American lookback options numerically. Secondly, to verify the pricing accuracy of the approximated solutions that we have derived, we implement the Monte-Carlo simulation. Comparing our analytic form formulas with the solutions obtained by the Monte-Carlo simulation with respect to the number of simulations, we demonstrate the usefulness of the option pricing with SV model. Finally, we investigate the numerical implications of the SV model on the American Lookback option in terms of several model parameters. We observe the quantitative and qualitative influences of the correction price on the American lookback options by examining the fast mean-reverting factor included in SV model. In other words, the quite interesting and delicate results can be drawn regarding the effect of the addition of SV to the BS model. It can be seen that the sensitivity of SV has a significant effect on the behaviors of some parameters or variable.

The remainder of this paper is organized as follows. In Section 2, we construct the underlying asset model under the SV model driven by the fast mean-reverting Ornstein-Uhlenbeck process and formulate the free boundary problems of American lookback options. Section 3 applies the asymptotic analysis and LCT to the PDEs for the option price to obtain the approximated closed solutions of the option price and the free boundary value for the derived PDEs. In Section 4, we analyze the influence of the value of the American lookback option under SV and investigate the sensitivities of the nature of the SV on the option price with regard to the model parameters. Moreover, we demonstrate the price accuracy of the American lookback option using the SV model by comparing the approximated option price with the Monte Carlo price. Section 5 presents concluding remarks.

2. Model formulation

2.1. The review of American lookback options: The case of the constant volatility

In this section, first of all, we review briefly the American lookback options with the constant volatility as shown in Dai and Kwok [10]. If S_t denote the price of the underlying asset of the lookback option, then the model dynamics under the real probability measure \mathbb{P} is given by

$$dS_t = (\mu - q)S_t dt + f(Y_t)S_t dW_t^s,$$

where μ and q are the return rate and dividend rate, respectively, and W_t^s is a standard Brownian motion. By using Girsanov theorem, the stochastic dynamics of the underlying asset price S_t follows

$$dS_t = (r - q)S_t dt + f(Y_t)S_t dW_t^{s*},$$

under the risk-neutral probability measure \mathbb{P}^* , where r is a risk-free interest rate and W_t^{s*} is the standard Brownian motion in \mathbb{P}^* .

If M is the realized maximum value of the asset price over the lookback monitoring period, then the no-arbitrage price of the American floating strike lookback put option is expressed by

$$P(t, s, m) = \sup_{\xi \in \Gamma[t, T]} \mathbb{E}^* [e^{-r(\xi-t)} h_1(S_\xi, M_\xi) | S_t = s, M_t = m],$$

where $h_1(S_\xi, M_\xi) = M_\xi - S_\xi$ is the payoff function, $\Gamma[t, T]$ is the set of stopping times ξ in $[t, T]$, and M_t is the maximum value process defined by $M_t = \max_{0 \leq \tau \leq t} S_\tau$.

In order to examine the early exercise boundaries and pricing behaviors of one-asset American options with lookback payoff, we consider the following linear complementarity formulation

$$(1) \quad \frac{\partial P}{\partial \tau} + \mathcal{L}P > 0, \quad P(t, s, m) > m - s, \quad \left(\frac{\partial P}{\partial t} + \mathcal{L}P \right) (P - (m - s)) = 0$$

with auxiliary conditions

$$(2) \quad \left. \frac{\partial P}{\partial m} \right|_{s=m} = 0, \quad P(T, s, m) = m - s, \quad P(t, s^*, m) = m - s^*, \quad \left. \frac{\partial P}{\partial s} \right|_{s=s^*} = -1,$$

where $m > s > 0$, $\tau = T - t$ and the operator \mathcal{L} is described by

$$\mathcal{L} = \frac{1}{2} \sigma^2 s^2 \frac{\partial^2}{\partial s^2} + (r - q)s \frac{\partial}{\partial s} - r\mathcal{I}.$$

Since the closed-form solutions for the linear complementarity problem (1) and (2) do not exist, Dai and Kwok [10] analyzed the optimal exercise policies and the price impact of American lookback options in case of the constant volatility by solving the optimal boundary problems (1) and (2) numerically. We can investigate the numerical results from Dai and Kwok [10].

Based on the stochastic nature of the volatility verified by the empirical studies for the historical data in the real financial market, in the next subsection, we are attempting to construct the model dynamics for American lookback options with stochastic volatility mentioned in Fouque et al. [17]. However, in our article, the techniques for solving the optimal exercise boundary problems are quite different from those in Dai and Kwok [10]. To derive the analytic solutions from the given linear complementarity problem numerically, we utilize Laplace-Carson transform which will present in Subsection 2.3.

2.2. Problem formulation

Next, referring to Fouque et al. [17], this subsection deals with the underlying asset pricing model, in which volatility is driven by a fast mean-reverting Ornstein-Uhlenbeck (OU) process. Let us consider the value S_t of the underlying asset that follows the stochastic differential equations (SDEs) described by

$$(3) \quad \begin{aligned} dS_t &= (\mu - q)S_t dt + f(Y_t)S_t dW_t^s, \\ dY_t &= \alpha(\theta - Y_t)dt + \beta dW_t^y, \end{aligned}$$

under a market probability measure \mathbb{P} , where μ and q are given by Subsection 2.1, and θ , α , and β are constants. In addition, f is a smooth function with $0 < c_1 \leq f \leq c_2 < \infty$ for some constants c_1 and c_2 (cf. Karatzas and Shreve [22]), and W_t^s and W_t^y are the correlated Brownian motions satisfying $d\langle W^s, W^y \rangle_t = \rho dt$. In addition, we note that Y_t mentioned in (3) has a Gaussian process with a distribution expressed by $Y_t \sim \mathcal{N}(\theta + (Y_0 - \theta)e^{-\alpha t}, \nu^2(1 - e^{-2\alpha t}))$, where $\mathcal{N}(a, b)$ is defined as a normal distribution with mean a and variance b .

The process Y_t is an ergodic process whose the characteristic time gets back to the mean level of its invariant distribution with $\mathcal{N}(\theta, \nu^2)$, where $\nu = \beta/\sqrt{2\alpha}$ denotes the variance of the invariant distribution of Y_t . As α increases, process Y_t in (3) tends to revert to the long-run mean level θ , regardless of the time. Here, we call α the rate of mean-reversion and model (3) is called the mean-reverting Ornstein-Uhlenbeck (OU) process because the volatility is a monotonic function of a process Y_t , so that the drift draws it toward the mean value θ , and then the volatility gets closer to $f(\theta)$ approximately. If the mean reversion rate α goes to infinity, the underlying asset price S_t approaches the Black-Scholes model with constant volatility. From empirical stock price experiments based on **Standard and Poor's 500 index** in the real financial market, it can be observed that the volatility of the stock price returns to a specific mean as shown in Fouque et al. [13] and [14]. According to Fouque et al. [14], an empirical analysis of high-frequency S&P 500 index data exhibits that α is in fact large and that ν^2 is a stable $\mathcal{O}(1)$ constant. Moreover, one can observe that the volatility of stock prices fluctuates very quickly throughout the lifetime of financial instruments, verifying volatility is well-modeled as a fast mean-reverting stochastic process. Thus, from this observation of volatility, if we introduce a parameter, ϵ , represented by the inverse of the mean

reversion rate α satisfying $\epsilon = 1/\alpha$, we can assume that the positive parameter ϵ is assumed to be small such that Y_t becomes a fast mean-reverting process.

Now, under an equivalent martingale measure \mathbb{P}^* , by using the Girsanov theorem, the model dynamics described in (3) can be converted into the following SDEs:

$$\begin{aligned} dS_t &= (r - q)S_t dt + f(Y_t)S_t dW_t^{s*}, \\ dY_t &= \left(\frac{1}{\epsilon}(\theta - Y_t) - \frac{v\sqrt{2}}{\sqrt{\epsilon}}\Lambda(Y_t) \right) dt + \frac{\nu\sqrt{2}}{\sqrt{\epsilon}} dW_t^{y*}, \end{aligned}$$

where $r > 0$ is a risk free interest rate, and the processes W_t^{s*} and W_t^{y*} are the transformed standard Brownian motions under a risk neutral measure \mathbb{P}^* , which satisfy the correlation $d\langle W^{s*}, W^{y*} \rangle_t = \rho dt$, where $W_t^{s*} = W_t^s + \int_0^t \frac{\mu-r}{f(Y_s)} ds$ and $W_t^{y*} = W_t^y + \int_0^t \gamma(Y_s) ds$, and $\left(\frac{\mu-r}{f(Y_s)}, \gamma(Y_s) \right)$ satisfies the Novikov condition. Here, we assume that γ is a smooth bounded function of y , and $\Lambda(Y_t)$ is the market price of the volatility risk expressed by $\Lambda(Y_t) = \rho \frac{\mu-r}{f(Y_t)} + \gamma(Y_t)\sqrt{1 - \rho^2}$.

Under the equivalent martingale measure, no-arbitrage pricing theory illustrates that option prices are the expectations of discounted payoffs with regard to a risk-neutral measure. Under the equivalent martingale measure \mathbb{P}^* , the no-arbitrage price of an American lookback put option is described by the following expectation representation:

$$(4) \quad P(t, s, m, y) = \sup_{\xi \in \Gamma[t, T]} \mathbb{E}^*[e^{-r(\xi-t)} h_2(S_\xi, M_\xi) \mid S_t = s, M_t = m, Y_t = y],$$

where $h_2(S_\xi, M_\xi) = M_\xi - S_\xi$ is the payoff function.

Before we deal with the optimal stopping problem (4), we consider the region of the optimal points (t, S_t) for which early exercise before the expiration date is optimal. If we set $\mathcal{D} = \{(t, s, m, y) \mid 0 \leq t < T, 0 < s < m, 0 < y, m < \infty\}$, then it can be divided into the exercise region \mathcal{E} and the continuation region \mathcal{C} defined by

$$\begin{aligned} \mathcal{E} &= \{(t, s, m, y) \mid P(t, s, m, y) = m - s\}, \\ \mathcal{C} &= \{(t, s, m, y) \mid P(t, s, m, y) > m - s\}, \end{aligned}$$

respectively. Then, there exists a boundary $s^* = s^*(t, y, m)$ that separates \mathcal{C} from \mathcal{E} , which we call the free boundary of an American lookback option, which is described by

$$(5) \quad s^*(t, y, m) = \inf\{s \mid (t, s, m, y) \in \mathcal{C}\}.$$

Lemma 2.1. *From the point of view of this expression of the early exercise boundary s^* , we can rewrite the two regions \mathcal{E} and \mathcal{C} as*

$$\mathcal{E} = \{(t, s, m, y) \mid 0 < s \leq s^*\} \text{ and } \mathcal{C} = \{(t, s, m, y) \mid s^* < s < m\},$$

respectively. Using a standard theory for the optimal stopping problem stated in [11], $P(t, s, m, y)$ yields the following variational inequality:

$$(6) \quad \begin{aligned} \frac{\partial P}{\partial t} + \mathcal{L}^\epsilon P &\leq 0, & \text{if } P(t, s, m, y) = m - s, \\ \frac{\partial P}{\partial t} + \mathcal{L}^\epsilon P &= 0, & \text{if } P(t, s, m, y) > m - s \end{aligned}$$

with one terminal condition $P(T, s, m, y) = m - s$, and four boundary conditions

$$(7) \quad \left. \frac{\partial P}{\partial m} \right|_{s=m} = 0, \quad P(t, s^*, m, y) = m - s^*, \quad \left. \frac{\partial P}{\partial s} \right|_{s=s^*} = -1, \quad \left. \frac{\partial P}{\partial y} \right|_{s=s^*} = 0$$

on the domain \mathcal{D} mentioned above, denoting that

- $P(t, s^*, m, y) = m - s^*$ (matching condition),
- $\left. \frac{\partial P}{\partial s} \right|_{s=s^*} = -1$ (smooth pasting condition with respect to s),
- $\left. \frac{\partial P}{\partial y} \right|_{s=s^*} = 0$ (smooth pasting condition with respect to y),

where

$$\begin{aligned} \mathcal{L}^\epsilon &= \frac{1}{2} f(y)^2 s^2 \frac{\partial^2}{\partial s^2} + (r - q) s \frac{\partial}{\partial s} - r\mathcal{I} + \rho \frac{\nu\sqrt{2}}{\sqrt{\epsilon}} s f(y) \frac{\partial^2}{\partial s \partial y} + \frac{\nu^2}{\epsilon} \frac{\partial^2}{\partial y^2} \\ &\quad + \left(\frac{1}{\epsilon} (\theta - y) - \frac{\nu\sqrt{2}}{\sqrt{\epsilon}} \Lambda(y) \right) \frac{\partial}{\partial y}. \end{aligned}$$

Proof. Referring to [11]. □

2.3. Review of Laplace-Carson transform

In this subsection, we present a review of the Laplace-Carson transform (LCT). The transform plays an important role in dealing with PDE problems by converting the related partial differential equations (PDEs) into ordinary differential equations (ODEs). The definition is as follows: for a continuous real-valued function $\chi(\tau)$ satisfying $|\chi(\tau)| \leq Ae^{B\tau}$ for constants A and B on a non-negative real number set $\mathbb{R}^+ \cup \{0\}$, the LCT of function χ is given by

$$\mathcal{LC} [\chi(\tau)] (\lambda) = \int_0^{+\infty} \lambda e^{-\lambda\tau} \chi(\tau) \, d\tau$$

for $\lambda \in \mathbb{C}$, and $\text{Re}(\lambda) > B$. We denote $\mathcal{LC} [\chi(\tau)] (\lambda) = \chi^*(\lambda)$ for simplicity, and for a random variable $X \sim \text{Exp}(\lambda)$, the LCT can be expressed as $\chi^*(\lambda) = \mathbb{E}[\chi(X)]$. We briefly describe some of the basic properties of the LCT in Appendix A.

3. Price approximation

In this section, we utilize an asymptotic analysis suggested by Fouque et al. [17] and LCT given in Subsection 2.3 to derive the PDEs for approximate solutions of the linear complementarity problem (6)-(7). Before implementing this procedure, we use the method of dimension reduction used in the studies of Dai [9] and Dai and Kwok [10] in equations (6) and (7). We denote $x, x^*(t, y)$, and $Q(t, x, y)$ as

$$x = \frac{s}{m}, \quad x^*(t, y) = \frac{s^*(t, m, y)}{m}, \quad \text{and} \quad Q(t, x, y) = \frac{P(t, s, m, y)}{m}$$

respectively.

Then, we obtain the transformed linear complementarity problems with a final condition and three boundary conditions as follows:

$$(8) \quad \begin{cases} \frac{\partial Q}{\partial t} + \tilde{\mathcal{L}}^\epsilon Q \leq 0, & \text{if } Q(t, x, y) = 1 - x, \\ \frac{\partial Q}{\partial t} + \tilde{\mathcal{L}}^\epsilon Q = 0, & \text{if } Q(t, x, y) > 1 - x, \\ \frac{\partial Q}{\partial x}(t, 1, y) = Q(t, 1, y), \quad Q(T, x, y) = 1 - x, \quad Q(t, x^*, y) = 1 - x^*, \\ \frac{\partial Q}{\partial x}|_{x=x^*} = -1, \quad \frac{\partial Q}{\partial y}|_{x=x^*} = 0 \end{cases}$$

on $\mathcal{D}^* = \mathcal{E}^* \cup \mathcal{C}^*$, where the transferred domains $\mathcal{E}^* = \{(t, x, y) | 0 < x \leq x^*(t, y)\}$ and $\mathcal{C}^* = \{(t, x, y) | x^*(t, y) < x < 1\}$, and the differential operator $\tilde{\mathcal{L}}^\epsilon$ are described by

$$\begin{aligned} \tilde{\mathcal{L}}^\epsilon = & \frac{1}{2}f(y)^2x^2\frac{\partial^2}{\partial x^2} + (r - q)x\frac{\partial}{\partial x} - r\mathcal{I} + \rho\frac{\nu\sqrt{2}}{\sqrt{\epsilon}}xf(y)\frac{\partial^2}{\partial x\partial y} + \frac{\nu^2}{\epsilon}\frac{\partial^2}{\partial x^2} \\ & + \left(\frac{1}{\epsilon}(\theta - y) - \frac{\nu\sqrt{2}}{\sqrt{\epsilon}}\Lambda(y)\right)\frac{\partial}{\partial y}. \end{aligned}$$

Now, to deal with the PDE problems (8) more easily, if we follow Tao [32] on the option price $Q(t, x, y)$ and consider the time-reversed processes defined by $\tilde{Q}(\tau, x, y) := Q(T - t, x, y) = Q(t, x, y)$ and $\tilde{x}^*(\tau, y) := x^*(T - t, y) = x^*(t, y)$, then the linear complementarity problems of $Q(t, x, y)$ mentioned in (8) can be converted into the following free boundary value problems.

$$(9) \quad \begin{cases} \tilde{Q}(\tau, x, y) = 1 - x, & \forall (x, y) \in (0, \tilde{x}^*] \times (-\infty, +\infty), \\ -\frac{\partial \tilde{Q}}{\partial \tau} + \tilde{\mathcal{L}}^\epsilon \tilde{Q} = 0, & \forall (x, y) \in (\tilde{x}^*, 1) \times (-\infty, +\infty), \\ \frac{\partial \tilde{Q}}{\partial x}(\tau, 1, y) = \tilde{Q}(\tau, 1, y), \quad \tilde{Q}(0, x, y) = 1 - x, \quad \tilde{Q}(\tau, \tilde{x}^*, y) = 1 - \tilde{x}^*, \\ \frac{\partial \tilde{Q}}{\partial x}(\tau, \tilde{x}^*, y) = -1, \quad \frac{\partial \tilde{Q}}{\partial y}(\tau, \tilde{x}^*, y) = 0. \end{cases}$$

To solve the PDE problem (9), we first decompose the differential operator $\tilde{\mathcal{L}}^\epsilon$ into

$$\tilde{\mathcal{L}}^\epsilon = \frac{1}{\epsilon}\mathcal{L}_0 + \frac{1}{\sqrt{\epsilon}}\mathcal{L}_1 + \mathcal{L}_2,$$

where

$$\begin{aligned}
 \mathcal{L}_0 &:= \nu^2 \frac{\partial}{\partial y^2} + (\theta - y) \frac{\partial}{\partial y}, \\
 \mathcal{L}_1 &:= \sqrt{2} \rho \nu x f(y) \frac{\partial^2}{\partial x \partial y} - \sqrt{2} \nu \Lambda(y) \frac{\partial}{\partial y}, \\
 \mathcal{L}_2 &:= \frac{1}{2} f(y)^2 x^2 \frac{\partial^2}{\partial x^2} + (r - q) x \frac{\partial}{\partial x} - r \mathcal{I},
 \end{aligned}
 \tag{10}$$

and in (10), we note that \mathcal{L}_0 is the infinitesimal generator of the mean-reverting OU process scaled by $\frac{1}{\alpha}$, \mathcal{L}_1 contains the mixed partial derivative owing to the correlation between the two Brownian motions and the first-order partial derivative from the market price of risk γ , and \mathcal{L}_2 is the Black-Scholes operator with the volatility level $f(y)$ excluding the time term.

If we expand $\tilde{Q}(\tau, x, y)$ and $\tilde{x}^*(\tau, y)$ in the PDE (9) by using the asymptotic series in terms of the small parameter $\sqrt{\epsilon}$, then $\tilde{Q}(\tau, x, y)$ and $\tilde{x}^*(\tau, y)$ are given by

$$\begin{aligned}
 \tilde{Q}(\tau, x, y) &= \sum_{n \geq 0} \epsilon^{n/2} \tilde{Q}_n(\tau, x, y), \\
 \tilde{x}^*(\tau, y) &= \sum_{n \geq 0} \epsilon^{n/2} \tilde{x}_n^*(\tau, y).
 \end{aligned}
 \tag{11}$$

Applying the LCT to (11) leads to

$$\begin{aligned}
 \hat{Q}(\lambda, x, y) &= \sum_{n \geq 0} \epsilon^{n/2} \hat{Q}_n(\lambda, x, y), \\
 \hat{x}(\lambda, y) &= \sum_{n \geq 0} \epsilon^{n/2} \hat{x}_n(\lambda, y),
 \end{aligned}
 \tag{12}$$

where $\hat{Q}(\lambda, x, y) = \mathcal{L}\mathcal{C}(\tilde{Q}(\tau, x, y))(\lambda)$, $\hat{Q}_n(\lambda, x, y) = \mathcal{L}\mathcal{C}(\tilde{Q}_n(\tau, x, y))(\lambda)$, $\hat{x}(\lambda, y) = \mathcal{L}\mathcal{C}(\tilde{x}^*(\tau, y))(\lambda)$ and $\hat{x}_n(\lambda, y) = \mathcal{L}\mathcal{C}(\tilde{x}_n^*(\tau, y))(\lambda)$, and the PDEs (9) are transformed into

$$(13) \quad \begin{cases} \hat{Q}(\lambda, x, y) = 1 - x, \quad \forall (x, y) \in (0, \hat{x}] \times (-\infty, +\infty), \\ \left(\frac{1}{\epsilon} \mathcal{L}_0 + \frac{1}{\sqrt{\epsilon}} \mathcal{L}_1 + \tilde{\mathcal{L}}_2\right) \hat{Q} + \lambda(1 - x) = 0, \quad \forall (x, y) \in (\hat{x}, 1) \times (-\infty, +\infty), \\ \frac{\partial \hat{Q}}{\partial x}(\lambda, 1, y) = \hat{Q}(\lambda, 1, y), \quad \hat{Q}(\lambda, \hat{x}, y) = 1 - \hat{x}, \\ \frac{\partial \hat{Q}}{\partial x}(\lambda, \hat{x}, y) = -1, \quad \frac{\partial \hat{Q}}{\partial y}(\lambda, \hat{x}, y) = 0, \end{cases}$$

where $\tilde{\mathcal{L}}_2 := \frac{1}{2} f(y)^2 x^2 \frac{\partial^2}{\partial x^2} + (r - q) x \frac{\partial}{\partial x} - (r + \lambda) \mathcal{I}$.

By applying the expansion of (12) to the boundary conditions $\frac{\partial \hat{Q}}{\partial x}(\lambda, 1, y) = \hat{Q}(\lambda, 1, y)$, $\hat{Q}(\lambda, \hat{x}, y) = 1 - \hat{x}$ and $\frac{\partial \hat{Q}}{\partial x}(\lambda, \hat{x}, y) = -1$ in (13), and using the Taylor

expansion around $x = \hat{x}_0$, we obtain the following relations with respect to $\sqrt{\epsilon}$:

$$\begin{aligned}
 & \left(\frac{\partial \hat{Q}_0}{\partial x}(\lambda, 1, y) - \hat{Q}_0(\lambda, 1, y) \right) + \sqrt{\epsilon} \left(\frac{\partial \hat{Q}_1}{\partial x}(\lambda, 1, y) - \hat{Q}_1(\lambda, 1, y) \right) + \dots = 0, \\
 (14) \quad & \hat{Q}_0(\lambda, \hat{x}_0, y) + \sqrt{\epsilon} \left(\hat{x}_1 \frac{\partial \hat{Q}_0}{\partial x}(\lambda, \hat{x}_0, y) + \hat{Q}_1(\lambda, \hat{x}_0, y) \right) + \dots = 1 - \hat{x}_0 - \sqrt{\epsilon} \hat{x}_1 + \dots, \\
 & \frac{\partial \hat{Q}_0}{\partial x}(\lambda, \hat{x}_0, y) + \sqrt{\epsilon} \left(\hat{x}_1 \frac{\partial^2 \hat{Q}_0}{\partial x^2}(\lambda, \hat{x}_0, y) + \frac{\partial \hat{Q}_1}{\partial x}(\lambda, \hat{x}_0, y) \right) + \dots = -1,
 \end{aligned}$$

where $\hat{x}_0 = \hat{x}_0(\lambda, y)$ and $\hat{x}_1 = \hat{x}_1(\lambda, y)$ are functions of λ and y , respectively.

In addition, from the expansion of \hat{Q} mentioned in (12), the PDE in (13) becomes

$$\begin{aligned}
 (15) \quad & \frac{1}{\epsilon} \mathcal{L}_0 \hat{Q}_0 + \frac{1}{\sqrt{\epsilon}} \left(\mathcal{L}_0 \hat{Q}_1 + \mathcal{L}_1 \hat{Q}_0 \right) + \left(\mathcal{L}_0 \hat{Q}_2 + \mathcal{L}_1 \hat{Q}_1 + \tilde{\mathcal{L}}_2 \hat{Q}_0 + \lambda(1 - x) \right) \\
 & + \sqrt{\epsilon} \left(\mathcal{L}_0 \hat{Q}_3 + \mathcal{L}_1 \hat{Q}_2 + \tilde{\mathcal{L}}_2 \hat{Q}_1 \right) + \dots = 0,
 \end{aligned}$$

and we have the following procedures from (15) to obtain the explicit-closed solutions for \hat{Q}_0 and \hat{Q}_1 :

• **The $\frac{1}{\epsilon}$ -order term:** Comparing the terms of order $\frac{1}{\epsilon}$ on both sides in (15), we have $\mathcal{L}_0 \hat{Q}_0(\lambda, x, y) = 0$, as shown in Theorem 4.1, as described in Choi et al. [5], if we assume that \hat{Q}_0 does not grow as much as $\frac{\partial \hat{Q}_0}{\partial y} \sim e^{y^2}$ as $y \rightarrow \infty$, then it implies $\hat{Q}_0 = \hat{Q}_0(\lambda, x)$. Thus, \hat{Q}_0 satisfies: $\mathcal{L}_0 \hat{Q}_0 = 0$ for $x > \hat{x}_0$, with the boundary condition $\hat{Q}_0(\lambda, \hat{x}_0) = 1 - \hat{x}_0$ and $\partial_x \hat{Q}_0(\lambda, \hat{x}_0) = -1$. In addition, because \hat{Q}_0 does not rely on y on each side of \hat{x}_0 , \hat{x}_0 are independent of y . That is, the PDE problem for \hat{Q}_0 yields

$$\begin{cases} \mathcal{L}_0 \hat{Q}_0(\lambda, x) = 0 \quad \forall x \in (\hat{x}_0, 1), \\ \hat{Q}_0(\lambda, x) = 1 - x \quad \forall x \in (0, \hat{x}_0], \\ \hat{Q}_0(\lambda, \hat{x}_0) = 1 - \hat{x}_0, \\ \frac{\partial \hat{Q}_0}{\partial x} \Big|_{x=\hat{x}_0} = -1, \quad \frac{\partial \hat{Q}_0}{\partial x}(\lambda, 1) = \hat{Q}_0(\lambda, 1). \end{cases}$$

• **The $\frac{1}{\sqrt{\epsilon}}$ -order term:** Comparing the terms of order $\frac{1}{\sqrt{\epsilon}}$ on both sides in (15), we obtain $\mathcal{L}_0 \hat{Q}_1 + \mathcal{L}_1 \hat{Q}_0 = 0$, and then it leads to $\mathcal{L}_1 \hat{Q}_0 = 0$ as all of two terms of \mathcal{L}_1 have the derivatives with respect to y . Therefore, we have $\mathcal{L}_0 \hat{Q}_1 = 0$, and assuming that \hat{Q}_1 does not grow as much as $\frac{\partial \hat{Q}_1}{\partial y} \sim e^{y^2}$ as $y \rightarrow \infty$, $\hat{Q}_1 = \hat{Q}_1(\lambda, x)$ holds. Similarly, \hat{x}_1 is independent of y . By using the relations stated in (14), the \hat{Q}_1 satisfies

$$\begin{cases} \mathcal{L}_1 \hat{Q}_0 + \mathcal{L}_0 \hat{Q}_1 = 0 \quad \forall x \in (\hat{x}_0, 1), \\ \hat{Q}_1(\lambda, x) = 0, \quad \forall x \in (0, \hat{x}_0], \\ \hat{x}_1(\lambda, y) \frac{\partial \hat{Q}_0}{\partial x}(\lambda, \hat{x}_0) + \frac{\partial \hat{Q}_1}{\partial x}(\lambda, \hat{x}_0) = 0, \\ \frac{\partial \hat{Q}_1}{\partial x}(\lambda, 1) = \hat{Q}_1(\lambda, 1). \end{cases}$$

• **The zero-order term:** In (15), the zero-order term comes up with $\mathcal{L}_0\hat{Q}_2 + \mathcal{L}_1\hat{Q}_1 + \tilde{\mathcal{L}}_2\hat{Q}_0 + \lambda(1-x) = 0$, because \hat{Q}_1 is independent of y , it is reduced to

$$(16) \quad \mathcal{L}_0\hat{Q}_2 + \tilde{\mathcal{L}}_2\hat{Q}_0 + \lambda(1-x) = 0.$$

Here, as we can regard $\tilde{\mathcal{L}}_2\hat{Q}_0 + \lambda(1-x)$ as a function of the variable y , equation (16) is of the form

$$\mathcal{L}_0\hat{Q}_2 + g(y) = 0,$$

which is well known as a *Poisson equation* with respect to the operator \mathcal{L}_0 in the variable y , where $g(y) = \tilde{\mathcal{L}}_2\hat{Q}_0 + \lambda(1-x)$. Applying *Fredholm alternative theorem* [30] to equation (16) guarantees that there is no solution to equation (16) if $g(y)$ is not centered on the invariant distribution of the Markov process Y whose infinitesimal generator is \mathcal{L}_0 . The centering condition is given by

$$\langle g \rangle = \int_{\mathbb{R}} g(y) \Phi(y) dy = 0,$$

where $\Phi(y) = \frac{1}{\sqrt{2\pi\nu}} \exp(-\frac{(y-\theta)^2}{2\nu^2})$ is the invariant distribution of Y with respect to the L^2 -inner product. So, the equation (16) satisfies the centering condition, it leads to

$$(17) \quad \begin{aligned} \langle \tilde{\mathcal{L}}_2\hat{Q}_0 + \lambda(1-x) \rangle &= \langle \tilde{\mathcal{L}}_2 \rangle \hat{Q}_0(\lambda, x) + \lambda(1-x) \\ &= \tilde{\mathcal{L}}_2(\bar{\sigma}) \hat{Q}_0(\lambda, x) + \lambda(1-x) = 0, \end{aligned}$$

where $\tilde{\mathcal{L}}_2(\bar{\sigma}) = \frac{1}{2}\bar{\sigma}^2 x^2 \frac{\partial^2}{\partial x^2} + (r-q)x \frac{\partial}{\partial x} - (r+\lambda)\mathcal{I}$ is the Black-Scholes operator with the effective volatility $\bar{\sigma}$ denoted by $\bar{\sigma}^2 = \langle f^2 \rangle$, as mentioned by Fouque et al. [17]. From (17), we have

$$\begin{aligned} \tilde{\mathcal{L}}_2\hat{Q}_0 + \lambda(1-x) &= \tilde{\mathcal{L}}_2\hat{Q}_0 + \lambda(1-x) - \langle \tilde{\mathcal{L}}_2\hat{Q}_0 + \lambda(1-x) \rangle \\ &= \frac{1}{2}x^2(f^2 - \langle f^2 \rangle) \frac{\partial^2 \hat{Q}_0}{\partial x^2}. \end{aligned}$$

• **The $\sqrt{\epsilon}$ -order term:** The order term of $\sqrt{\epsilon}$ in (15) must also be equal to zero, yielding

$$(18) \quad \mathcal{L}_0\hat{Q}_3 + \mathcal{L}_1\hat{Q}_2 + \tilde{\mathcal{L}}_2\hat{Q}_1 = 0.$$

Regarding equation (18) as a Poisson equation for \hat{Q}_3 with respect to \mathcal{L}_0 and taking the average with respect to the invariant distribution of Y , we obtain

$$(19) \quad \langle \mathcal{L}_1\hat{Q}_2 + \tilde{\mathcal{L}}_2\hat{Q}_1 \rangle = 0.$$

Then, from the operators presented in (10) and (16), we obtain

$$\begin{aligned} \hat{Q}_2 &= -\mathcal{L}_0^{-1} \left(\tilde{\mathcal{L}}_2\hat{Q}_0 + \lambda(1-x) \right) \\ &= -\frac{1}{2}x^2 \mathcal{L}_0^{-1} (f^2 - \langle f^2 \rangle) \frac{\partial^2 \hat{Q}_0}{\partial x^2} = -\frac{1}{2} (\phi(y) + c(\lambda, x)) x^2 \frac{\partial^2 \hat{Q}_0}{\partial x^2}, \end{aligned}$$

where $\phi(y)$ is the solution of the Poisson equation $\mathcal{L}_0\phi = f(y)^2 - \langle f(y)^2 \rangle$ and $c(\lambda, x)$ is a function with regard to λ and x , and from (19), we deduce the non-homogeneous PDE

$$\begin{aligned}
 \tilde{\mathcal{L}}_2(\bar{\sigma})\hat{Q}_1 &= \left\langle \frac{1}{2} (\phi(y) + c(\lambda, x)) x^2 \frac{\partial^2 \hat{Q}_0}{\partial x^2} \right\rangle \\
 &= \frac{1}{2} \langle \mathcal{L}_1\phi(y) \rangle x^2 \frac{\partial^2 \hat{Q}_0}{\partial x^2} \\
 &= \frac{\sqrt{2}}{2} \rho \nu \langle f(y)\phi'(y) \rangle x^3 \frac{\partial^3 \hat{Q}_0}{\partial x^3} \\
 &\quad + \left(\sqrt{2} \rho \nu \langle f(y)\phi'(y) \rangle - \frac{\sqrt{2}}{2} \nu \langle \Lambda(y)\phi'(y) \rangle \right) x^2 \frac{\partial^2 \hat{Q}_0}{\partial x^2}.
 \end{aligned}
 \tag{20}$$

Therefore, from (17) and (20), \hat{Q}_0 and \hat{Q}_1 satisfy the following PDEs:

$$\begin{cases}
 \tilde{\mathcal{L}}_2(\bar{\sigma})\hat{Q}_0(\lambda, x) + \lambda(1 - x) = 0, & \forall x \in (\hat{x}_0, 1), \\
 \hat{Q}_0(\lambda, x) = 1 - x, & \forall x \in (0, \hat{x}_0], \\
 \frac{\partial \hat{Q}_0}{\partial x}(\lambda, 1) = \hat{Q}_0(\lambda, 1), \quad \hat{Q}_0(\lambda, \hat{x}_0) = 1 - \hat{x}_0, \quad \frac{\partial \hat{Q}_0}{\partial x}(\lambda, \hat{x}_0) = -1
 \end{cases}
 \tag{21}$$

and

$$\begin{cases}
 \tilde{\mathcal{L}}(\bar{\sigma})\hat{Q}_1(\lambda, x) = V_2 x^2 \frac{\partial^2 \hat{Q}_0}{\partial x^2} + V_3 x^3 \frac{\partial^3 \hat{Q}_0}{\partial x^3}, & \forall x \in (\hat{x}_0, 1), \\
 \hat{Q}_1(\lambda, x) = 0, & \forall x \in (0, \hat{x}_0], \\
 \frac{\partial \hat{Q}_1}{\partial x}(\lambda, 1) = \hat{Q}_1(\lambda, 1), \quad \hat{x}_1 = -\frac{\partial_x \hat{Q}_1}{\partial_{xx}^2 \hat{Q}_0}(\hat{x}_0),
 \end{cases}
 \tag{22}$$

respectively, where

$$\begin{aligned}
 V_2 &:= \sqrt{2} \rho \nu \langle f(y)\phi'(y) \rangle - \frac{\sqrt{2}}{2} \nu \langle \Lambda(y)\phi'(y) \rangle, \\
 V_3 &:= \frac{\sqrt{2}}{2} \rho \nu \langle f(y)\phi'(y) \rangle.
 \end{aligned}
 \tag{23}$$

4. Option price formulas

In this section, using the results discussed in the previous section and the inverse LCT, we derive the corrected option price which consists of the leading order term and the correction order term. In fact, the corrected option price is one of the main contributions in our study. Mathematically, it is expressed by

$$(\text{Corrected option price}) = (\text{leading order price}) + (\text{correction term}),$$

where (leading order price) = P_0 and (correction term) = $\sqrt{\epsilon}P_1$.

Theorem 4.1 (Value of the leading order term for the American lookback options in frequency domain). *If we solve the ODEs given by (21), then the*

value of the leading order term $\hat{Q}_0(\lambda, x)$ for the American lookback option is explicitly described by

$$\hat{Q}_0(\lambda, x) = \begin{cases} A_1 x^{a_1} + A_2 x^{a_2} - \frac{\lambda}{\lambda+q} x + \frac{\lambda}{\lambda+r}, & \forall x \in (\hat{x}_0, 1), \\ 1 - x, & \forall x \in (0, \hat{x}_0], \end{cases}$$

where the coefficients A_1 and A_2 are given by

$$A_1 = -\frac{\frac{\lambda}{\lambda+r} a_2 \hat{x}_0^{a_2} + \frac{q}{\lambda+q} \hat{x}_0 (a_2 - 1)}{a_1 (a_2 - 1) \hat{x}_0^{a_1} - a_2 (a_1 - 1) \hat{x}_0^{a_2}} \quad \text{and}$$

$$A_2 = \frac{\frac{\lambda}{\lambda+r} a_1 \hat{x}_0^{a_1} + \frac{q}{\lambda+q} \hat{x}_0 (a_1 - 1)}{a_1 (a_2 - 1) \hat{x}_0^{a_1} - a_2 (a_1 - 1) \hat{x}_0^{a_2}},$$

respectively. In addition, the free boundary value $\hat{x}_0 = \hat{x}_0(\lambda)$ is determined by the following algebraic equation:

$$\frac{\lambda}{\lambda+r} (a_1 - a_2) \hat{x}_0^{a_1} + \frac{q}{\lambda+q} \left(-(a_1 - 1)(a_2 - 1) \hat{x}_0 + (a_1 - 1)(a_2 - 1) \hat{x}_0^{a_1 - a_2 + 1} \right) - \frac{r}{\lambda+r} \left(a_1 (a_2 - 1) \hat{x}_0^{a_1 - a_2} - (a_1 - 1) a_2 \right) = 0.$$

Proof. In (21),

$$(24) \quad \tilde{\mathcal{L}}(\bar{\sigma}) \hat{Q}_0(\lambda, x) + \lambda(1 - x) = 0, \quad \forall x \in (\hat{x}_0, 1)$$

is a non-homogeneous Cauchy-Euler equation, and the characteristic equation for (24) is given by

$$(25) \quad \frac{1}{2} \bar{\sigma}^2 a^2 + \left(r - q - \frac{1}{2} \bar{\sigma}^2 \right) a - (r + \lambda) = 0.$$

Let us define $a_1 = a_1(\lambda) > 1$ and $a_2 = a_2(\lambda) < 0$ as two real roots of the quadratic equation (25). If we set $\hat{Q}_0(\lambda, x)$ by $\hat{Q}_0(\lambda, x) = A_1 x^{a_1} + A_2 x^{a_2} + A_3 x + A_4$, we can explicitly obtain the following closed solution.

$$(26) \quad \hat{Q}_0(\lambda, x) = A_1 x^{a_1} + A_2 x^{a_2} - \frac{\lambda}{\lambda+q} x + \frac{\lambda}{\lambda+r}.$$

To determine the constants A_1 and A_2 , we apply two conditions $\frac{\partial \hat{Q}_0}{\partial x}(\lambda, 1) = \hat{Q}_0(\lambda, 1)$ and $\frac{\partial \hat{Q}_0}{\partial x}(\lambda, \hat{x}_0) = -1$ to (26), we obtain

$$(27) \quad \begin{cases} (a_1 - 1)A_1 + (a_2 - 1)A_2 = \frac{\lambda}{\lambda+r}, \\ a_1 A_1 \hat{x}_0^{a_1} + a_2 A_2 \hat{x}_0^{a_2} = -\frac{q}{\lambda+q} \hat{x}_0. \end{cases}$$

Then

$$A_1 = -\frac{\frac{\lambda}{\lambda+r} a_2 \hat{x}_0^{a_2} + \frac{q}{\lambda+q} \hat{x}_0 (a_2 - 1)}{a_1 (a_2 - 1) \hat{x}_0^{a_1} - a_2 (a_1 - 1) \hat{x}_0^{a_2}} \quad \text{and}$$

$$A_2 = \frac{\frac{\lambda}{\lambda+r} a_1 \hat{x}_0^{a_1} + \frac{q}{\lambda+q} \hat{x}_0 (a_1 - 1)}{a_1 (a_2 - 1) \hat{x}_0^{a_1} - a_2 (a_1 - 1) \hat{x}_0^{a_2}}$$

are satisfied. Similarly, applying the condition $\hat{Q}_0(\lambda, \hat{x}_0) = 1 - \hat{x}_0$ to (27) leads to

$$A_1 \hat{x}_0^{a_1} + A_2 \hat{x}_0^{a_2} = \frac{r}{\lambda + r} - \frac{q}{\lambda + q} \hat{x}_0,$$

and it comes up with the following algebraic equation

$$\begin{aligned} & \frac{\lambda}{\lambda + r} (a_1 - a_2) \hat{x}_0^{a_1} + \frac{q}{\lambda + q} (-(a_1 - 1)(a_2 - 1) \hat{x}_0 + (a_1 - 1)(a_2 - 1) \hat{x}_0^{a_1 - a_2 + 1}) \\ & - \frac{r}{\lambda + r} (a_1(a_2 - 1) \hat{x}_0^{a_1 - a_2} - (a_1 - 1)a_2) = 0. \end{aligned}$$

Therefore, we derive the desired results for solutions \hat{Q}_0 and \hat{x}_0 . □

Theorem 4.2 (Value of the first-order correction term for the American lookback options in frequency domain). *From (22), the solution of the first-order correction term $\hat{Q}_1(\lambda, x)$ for American lookback options is described by*

$$\hat{Q}_1(\lambda, x) = (B_1 + C_1 \log x)x^{a_1} + (B_2 + C_2 \log x)x^{a_2},$$

and the correction term for the optimal exercise boundary is given by

$$\hat{x}_1 = \frac{(a_1 B_1 + C_1) \hat{x}_0^{a_1 - 1} + (a_2 B_2 + C_2) \hat{x}_0^{a_2 - 1} + a_1 C_1 \hat{x}_0^{a_1 - 1} \log \hat{x}_0 + a_2 C_2 \hat{x}_0^{a_2 - 1} \log \hat{x}_0}{a_1(a_1 - 1)A_1 \hat{x}_0^{a_1 - 2} + a_2(a_2 - 1)A_2 \hat{x}_0^{a_2 - 2}},$$

where

$$\begin{aligned} B_1 &= -\frac{-(C_1 + C_2) \hat{x}_0^{a_2} + (a_2 - 1)(C_1 \hat{x}_0^{a_1} \log \hat{x}_0 + C_2 \hat{x}_0^{a_2} \log \hat{x}_0)}{(a_1 - 1) \hat{x}_0^{a_2} - (a_2 - 1) \hat{x}_0^{a_1}}, \\ B_2 &= -\frac{-(C_1 + C_2) \hat{x}_0^{a_1} + (a_1 - 1)(C_1 \hat{x}_0^{a_1} \log \hat{x}_0 + C_2 \hat{x}_0^{a_2} \log \hat{x}_0)}{(a_1 - 1) \hat{x}_0^{a_1} - (a_2 - 1) \hat{x}_0^{a_2}}, \\ C_1 &= \frac{(V_2 + V_3(a_1 - 2)) A_1 a_1 (a_1 - 1)}{\frac{1}{2} \bar{\sigma}^2 (2a_1 - 1) + (r - q)}, \quad C_2 = \frac{(V_2 + V_3(a_2 - 2)) A_2 a_2 (a_2 - 1)}{\frac{1}{2} \bar{\sigma}^2 (2a_2 - 1) + (r - q)}. \end{aligned}$$

Proof. From (22),

$$(28) \quad \tilde{\mathcal{L}}(\bar{\sigma}) \hat{Q}_1(\lambda, x) = V_2 x^2 \frac{\partial^2 \hat{Q}_0}{\partial x^2} + V_3 x^3 \frac{\partial^3 \hat{Q}_0}{\partial x^3}, \quad x \in (\hat{x}_0, 1),$$

and suppose that $\hat{Q}_1(\lambda, x)$ is in the form of $\hat{Q}_1(\lambda, x) = (B_1 + C_1 \log x)x^{a_1} + (B_2 + C_2 \log x)x^{a_2}$. Applying the solution $\hat{Q}_0(\lambda, x)$ presented in Theorem 4.1, and $\hat{Q}_1(\lambda, x)$ to (28), we can rewrite equation (28) as

$$(29) \quad \begin{aligned} \text{(LHS)} &= \left(\frac{1}{2} \bar{\sigma}^2 (2a_1 - 1) + (r - q)\right) C_1 x^{a_1} + \left(\frac{1}{2} \bar{\sigma}^2 (2a_2 - 1) + (r - q)\right) C_2 x^{a_2}, \\ \text{(RHS)} &= (V_3(a_1 - 2) + V_2) A_1 a_1 (a_1 - 1) x^{a_1} + (V_3(a_2 - 2) + V_2) A_2 a_2 (a_2 - 1) x^{a_2}. \end{aligned}$$

By comparing the coefficients for x^{a_1} and x^{a_2} on both sides in (29), we obtain

$$\begin{aligned} C_1 &= \frac{(V_2 + V_3(a_1 - 2)) A_1 a_1 (a_1 - 1)}{\frac{1}{2} \bar{\sigma}^2 (2a_1 - 1) + (r - q)} \quad \text{and} \\ C_2 &= \frac{(V_2 + V_3(a_2 - 2)) A_2 a_2 (a_2 - 1)}{\frac{1}{2} \bar{\sigma}^2 (2a_2 - 1) + (r - q)}. \end{aligned}$$

From the two conditions $\frac{\partial \hat{Q}_1}{\partial x}(\lambda, 1) = \hat{Q}_1(\lambda, 1)$ and $\hat{Q}_1(\lambda, \hat{x}_0) = 0$, we have that

$$\begin{aligned} (a_1 - 1)B_1 + (a_2 - 1)B_2 + C_1 + C_2 &= 0, \\ \hat{x}_0^{a_1} B_1 + \hat{x}_0^{a_2} B_2 + \hat{x}_0^{a_1} \log(\hat{x}_0) C_1 + \hat{x}_0^{a_2} \log(\hat{x}_0) C_2 &= 0 \end{aligned}$$

and, if we solve the above simultaneous equations, then

$$\begin{aligned} B_1 &= -\frac{-(C_1 + C_2)\hat{x}_0^{a_2} + (a_2 - 1)(C_1\hat{x}_0^{a_1} \log \hat{x}_0 + C_2\hat{x}_0^{a_2} \log \hat{x}_0)}{(a_1 - 1)\hat{x}_0^{a_2} - (a_2 - 1)\hat{x}_0^{a_1}}, \\ B_2 &= -\frac{-(C_1 + C_2)\hat{x}_0^{a_1} + (a_1 - 1)(C_1\hat{x}_0^{a_1} \log \hat{x}_0 + C_2\hat{x}_0^{a_2} \log \hat{x}_0)}{(a_1 - 1)\hat{x}_0^{a_1} - (a_2 - 1)\hat{x}_0^{a_2}}. \end{aligned}$$

Finally, by using the condition $\hat{x}_1 = -\frac{\partial_x \hat{Q}_1}{\partial_{xx}^2 \hat{Q}_0}(\hat{x}_0)$, \hat{x}_1 can be explicitly calculated.

$$\hat{x}_1 = \frac{(a_1 B_1 + C_1)\hat{x}_0^{a_1-1} + (a_2 B_2 + C_2)\hat{x}_0^{a_2-1} + a_1 C_1 \hat{x}_0^{a_1-1} \log \hat{x}_0 + a_2 C_2 \hat{x}_0^{a_2-1} \log \hat{x}_0}{a_1(a_1 - 1)A_1 \hat{x}_0^{a_1-2} + a_2(a_2 - 1)A_2 \hat{x}_0^{a_2-2}}.$$

Therefore, we obtain the solutions of \hat{Q}_1 and \hat{x}_1 . □

As shown in Fouque et al. [17] or the procedures for the approximation mentioned in Section 3, using the expansions (11), the approximated (or analytic) solutions for \tilde{Q} in the PDEs (9) are given by

$$(30) \quad \tilde{Q}(\tau, x, y) \approx \tilde{Q}(\tau, x) = \tilde{Q}_0 + \sqrt{\epsilon} \tilde{Q}_1,$$

$$(31) \quad \tilde{x}^*(\tau, y) \approx \tilde{x}^*(\tau) = \tilde{x}_0^* + \sqrt{\epsilon} \tilde{x}_1^*.$$

However, because it is very difficult to solve \tilde{Q}_0 , \tilde{Q}_1 , \tilde{x}_0^* , and \tilde{x}_1^* directly in (30) and (31), we applied the LCT to the PDEs (9) to obtain the transformed PDEs stated in (13). Then, using the singular perturbation method, we obtain the explicit closed formulas for \hat{Q}_0 , \hat{Q}_1 , \hat{x}_0 , and \hat{x}_1 .

In the following process, we attempt to use the inverse LCT on the results obtained from Theorem 4.1 and Theorem 4.2 to derive the analytic formulas for the American lookback options using the SV model mentioned in (9). For the inversion of the LCT, we utilize the Gaver-Stehfest method proposed by Gaver [18] and Stehfest [31]. Therefore, we calculate the solution of $\tilde{Q}(\tau, x, y)$ mentioned in (9) numerically, which can be $\tilde{Q}(\tau, x) = \tilde{Q}_0 + \sqrt{\epsilon} \tilde{Q}_1$, by using the Laplace-Carson algorithm given by Gaver [18]. In other words, considering the speed and stability of the calculation, to obtain the desired approximated formulas $\tilde{Q}_0 + \sqrt{\epsilon} \tilde{Q}_1$, we use the n -th extrapolation Gaver-Stehfest methods. In particular, the Gaver-Stehfest method with 5-th extrapolation for pricing accuracy was used in this study. The brief illustrations for the inversion of the Gaver-Stehfest method are given in Appendix B.

Based on the numerical results for (30) and (31) implemented using the Gaver-Stehfest method, we have the first-order approximations of the American

lookback options $P(t, s, m, y)$ and $s^*(t, y, m)$ described by (4) and (5), which are defined as $\bar{P}(t, s, m)$ and $\bar{s}^*(t, m)$, respectively, given by

$$(32) \quad \begin{aligned} P(t, s, m, y) &\approx P_0(t, s, m) + \sqrt{\epsilon}P_1(t, s, m) := \bar{P}(t, s, m), \\ s^*(t, y, m) &\approx s_0(t, m) + \sqrt{\epsilon}s_1(t, m) = \bar{s}^*(t, m), \end{aligned}$$

where $P_0(t, s, m) = mQ_0(t, x) = m\tilde{Q}_0(\tau, x)$, $P_1(t, s, m) = mQ_1(t, x) = m\tilde{Q}_1(\tau, x)$, $s_0(t, m) = mx_0(t) = m\tilde{x}_0^*(\tau)$ and $s_1(t, m) = mx_1(t) = m\tilde{x}_1^*(\tau)$ as $Q(t, x, y) = \frac{P(t, s, m, y)}{m}$, where $x = \frac{s}{m}$. A detailed proof of the error accuracy of the first approximation expressed by (32) is presented by Fouque et al. [16,17]. In other words, from the asymptotic expansion method on the PDEs (9), if the payoff function h is smooth, then the accuracy of the first-order approximation is described by

$$\left| P(t, s, m, y) - [P_0(t, s, m) + \sqrt{\epsilon}P_1(t, s, m)] \right| \leq \mathcal{O}(\epsilon).$$

However, if the payoff function h does not have a smooth function, that is, h is not continuously differentiable, we need to proceed with the procedure for a payoff-regularization statement considering the pointwise accuracy of the corrected option price as the payoff function has an angle at the strike price. By utilizing the payoff regularization given by Fouque et al. [16], we can extend the accuracy of the first approximation in (32) by assuming that the maturity is $T - \delta$ in place of T . Then, the error accuracy of the first-order approximation in (32) is given by

$$\left| P(t, s, m, y) - [P_0(t, s, m) + \sqrt{\epsilon}P_1(t, s, m)] \right| \leq \mathcal{O}(\epsilon \ln \epsilon).$$

5. Numerical experiments

In this section, we investigate the impact of the price changes of the American lookback options and their optimal exercise boundaries under SV in terms of the model parameters. The numerical implications are carried out through the scaled approximated prices given by (30) and (31), obtained by the inversion of the Gaver-Stehfest method. The model parameters used in the numerical experiments are listed in Table 1.

TABLE 1. The parameters used for numerical analysis.

μ	θ	ν	ρ	ϵ	V_2	V_3
1.0	-2.5	1.0	-0.3	0.04	0.1203	0.0018

In the equations for universal group parameters V_2 and V_3 presented in (23), if we set $f(y)$ and $\Lambda(y)$ as $f(y) = e^y$ and $\Lambda(y) = e^{-y}$, respectively, then the effective volatility $\bar{\sigma} = \left(\int_{-\infty}^{\infty} f^2(y) \Phi(y) dy \right)^{1/2}$ is given by $e^{\theta + \nu^2}$. In

addition, $\phi(y)$ included in V_2 and V_2 is a solution of the second-order ODE $\mathcal{L}_0\phi = f(y)^2 - \bar{\sigma}^2$, and V_2 and V_3 described by Fouque et al. [17] using these specific functions gives

$$V_2 = \frac{1}{\sqrt{2\nu}} \left[2\rho e^{3\theta} \left(e^{5\nu^2/2} - e^{9\nu^2/2} \right) + \left(\rho(\mu-r) + \sqrt{1-\rho^2} \right) e^\theta \left(e^{5\nu^2/2} - e^{\nu^2/2} \right) \right],$$

$$V_3 = -\frac{\rho}{\sqrt{2\nu}} e^{3\theta} \left(e^{9\nu^2/2} - e^{5\nu^2/2} \right).$$

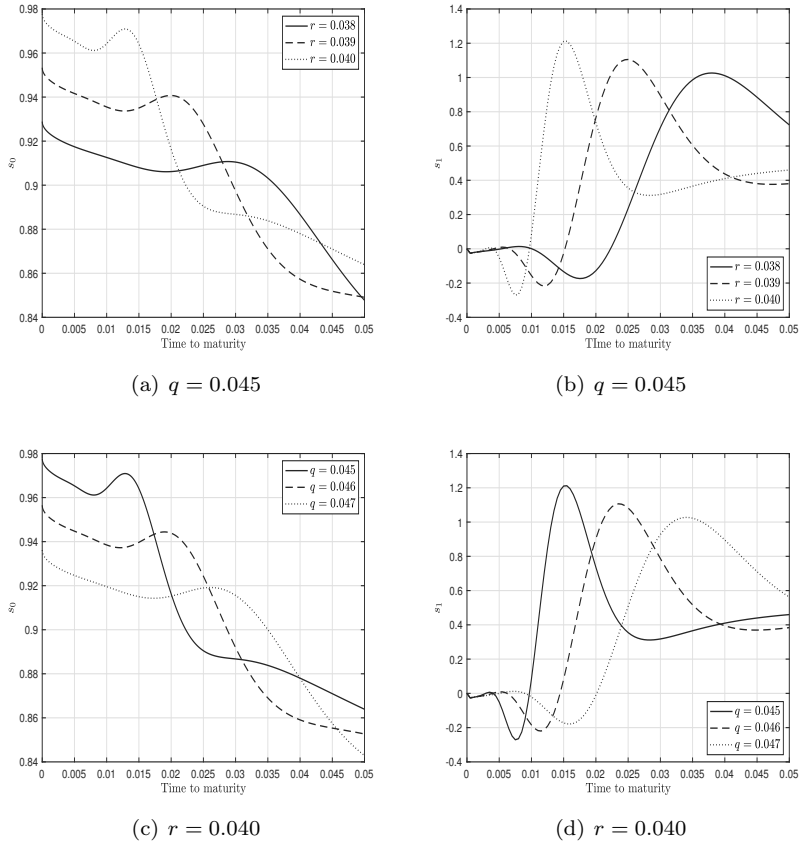


FIGURE 1. Optimal exercise values of the leading-order term $s_0(= m\tilde{x}_0^*)$ and correction term $s_1(= m\tilde{x}_1^*)$ based on dividend yield and interest rate.

Figure 1 plots the changes of the free-boundary values of the leading order s_0 and the correction order s_1 with respect to time-to-maturity for given dividend yields or interest rates. As shown in Figure 1(a) and Figure 1(c), as time to

maturity increases, the value of s_0 tends to decrease. Furthermore, in Figure 1(b) and Figure 1(d), we can observe that as time-to-maturity gets closer to 0, the price differences in s_1 for interest rates or dividend yields are insignificant or zero. It implies that the effects of the SV on the free boundary values are almost insignificant as time-to-maturity expires, while the influences of the SV on the free boundary prices become significant as the maturity is far in the future compared to the valuation time. Moreover, the price behaviors of the correction order term s_1 have a tendency to be larger than those of the leading order term s_0 in terms of time-to-maturity. It means that the impacts of the SV on the price of the optimal boundaries are very sensitive against time-to-maturity for given dividend rates or interest rates.

Figure 2 shows the price behaviors of the leading order term P_0 and the correction term P_1 with regard to the ratio of the underlying asset to the maximum process defined by $M_t = \max_{0 \leq \tau \leq t} S_\tau$. As shown in Figure 2, the leading-order price P_0 tends to decrease in terms of $\frac{s}{m}$. However, the correction price P_1 does not have any monotonicity, and in particular, has a hump phenomenon near $\frac{s}{m} = 0.96$. Furthermore, it can be observed that the sensitivity of the value of the correction term P_1 is much larger than that of the leading term P_0 . This implies that the price sensitivity of the SV on the American lookback options is significant in terms of the underlying asset or the maximum value process.

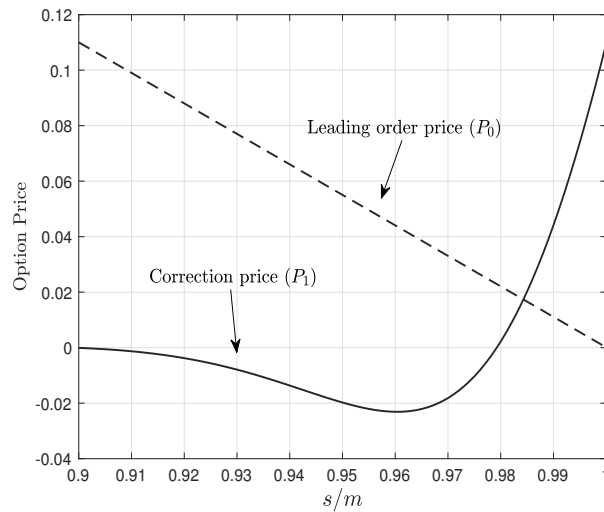
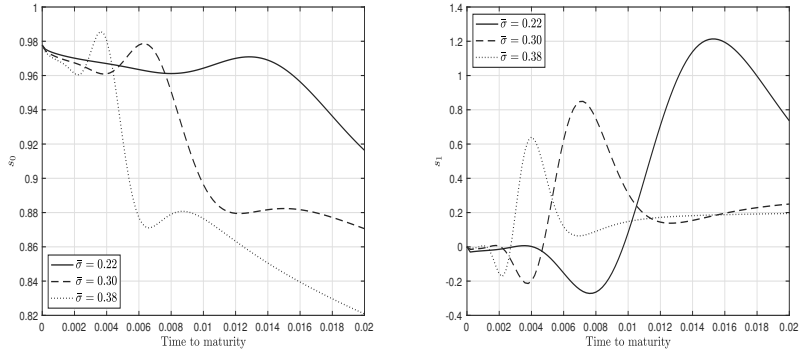
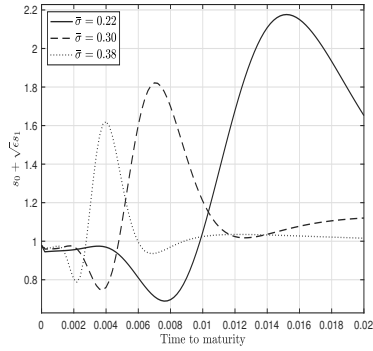


FIGURE 2. Graphs of the leading order price and correction price with respect to the ratio of the underlying asset to the maximum process defined by $M_t = \max_{0 \leq \tau \leq t} S_\tau$ ($r = 0.040$, $q = 0.045$ and $\tau = 0.02$).



(a) Value of the leading-order term of the free-boundary with respect to time-to-maturity with $\bar{\sigma} = 0.22, 0.30, 0.38$ (b) Value of the correction term of the free-boundary with respect to time-to-maturity with $\bar{\sigma} = 0.22, 0.30, 0.38$



(c) Value of the free-boundary with respect to time-to-maturity with $\bar{\sigma} = 0.22, 0.30, 0.38$

FIGURE 3. Value of the free-boundaries $s_0(= m\tilde{x}_0^*)$, $s_1(= m\tilde{x}_1^*)$ and $s_0 + \sqrt{\epsilon}s_1$ with regard to effective volatility ($r = 0.040, q = 0.045$).

Figure 3 depicts the price effect of the optimal boundary s_0 , the correction term s_1 , and the corrected term $s_0 + \sqrt{\epsilon}s_1$ with respect to the time-to-maturity for each effective volatility. Here, the standard of the choice is based on the direct computation from the model parameters given in Table 1, where the effective volatility is given by

$$\bar{\sigma} = \left(\int_{-\infty}^{\infty} f^2(y) \Phi(y) dy \right)^{\frac{1}{2}} = e^{\theta + \nu^2} \approx 0.22.$$

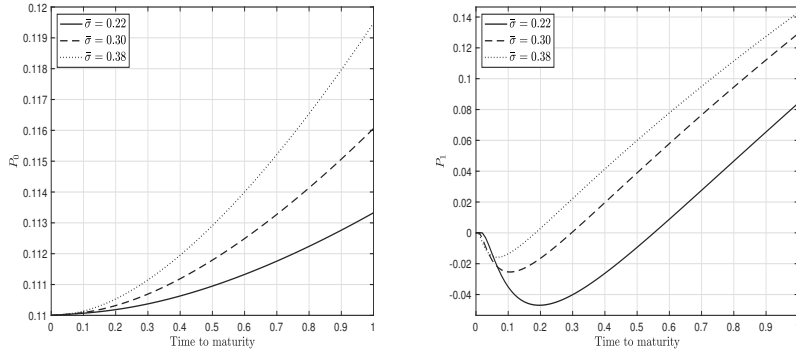
Therefore, to observe the price behaviors of the free boundaries for the effective volatilities, we take three effective volatilities at intervals of 0.8 from $\bar{\sigma} = 0.22$. Similar to Figure 1, the price influences of the optimal exercise boundaries s_1 are larger than those of s_0 in terms of time to maturity. This means that the effect of SV on the free-boundary value is more sensitive to that of the Black-Scholes (BS). In addition, in the case of the leading order price s_0 in Figure 3(a), it can be observed that the larger the effective volatility, the greater the impact on the free-boundary price. In contrast, in the case of the correction order price s_1 and the corrected price $s_0 + \sqrt{\epsilon}s_1$ stated in Figure 3(b) and Figure 3(c), respectively, it shows that if the effective volatility increases, the price change becomes more insignificant. It also implies that the free-boundary value s_0 is dominated by the free-boundary value s_1 , and eventually, the SV factor against the effective volatility exerts a significant effect on the value of the optimal boundary.

Figure 4 plots the changes of the option prices for P_0 , P_1 and $P_0 + \sqrt{\epsilon}P_1$ with regard to time-to-maturity for each effective volatility $\bar{\sigma}$. As seen in the Figure 4(a) and Figure 4(b), as the lines get closer to the maturity, the price gaps become zero for given effective volatilities. In addition, the price of the leading-order term P_0 is less sensitive to time-to-maturity compared with the correction term P_1 , and we can observe that the price changes of the correction term are much more significant compared with that of the leading-order term for the effective volatility as well as time-to-maturity, having a hump shape near the expiration. It implies that the option price is significantly affected by the SV factor with respect to time-to-maturity as well as the effective volatility.

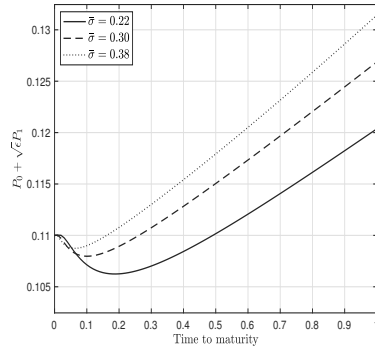
Figure 5 displays the price influences for P_0 , P_1 , and $P_0 + \sqrt{\epsilon}P_1$ in terms of the maximum process M for the given effective volatilities. Surprisingly, as shown in Figure 5(a), there is little or no change in the leading-order price P_0 for each effective volatility, while the correction price P_1 has a substantial change in the given effective volatility, giving rise to the hump phenomena similar to those in Figure 4. Thus, it can be observed that the nature of SV has a great effect on the American lookback options for effective volatility and the maximum process.

From now on, we make use of the analytical solution of the American lookback options expressed by (32) to examine the sensitivity of the option price in terms of the model parameters. The existence of this approximated solution allows us to contribute significantly to the efficiency and accuracy of the pricing of American lookback options. To demonstrate the accuracy of the approximated corrected solution described by (32), we compare our approximated formula with the numerical price obtained from a Monte Carlo simulation.

Tables 2 and 3 show the price differences between the solution of the Monte Carlo simulation and the approximated solution of the American lookback options according to the small parameter ϵ and the number of simulations, respectively. Referring to the calibrated parameters described by Fouque et al. [17] and [15], we carry out the Monte-Carlo simulation. All the computations for



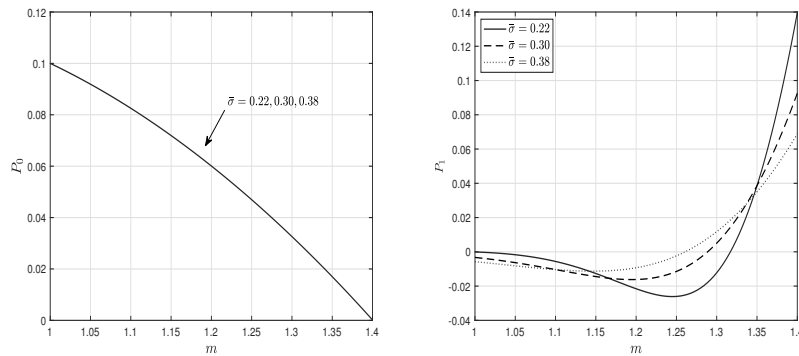
(a) Option value of the leading-order term with respect to time-to-maturity with $\bar{\sigma} = 0.22, 0.30, 0.38$
 (b) Option value of the correction term with respect to time-to-maturity with $\bar{\sigma} = 0.22, 0.30, 0.38$



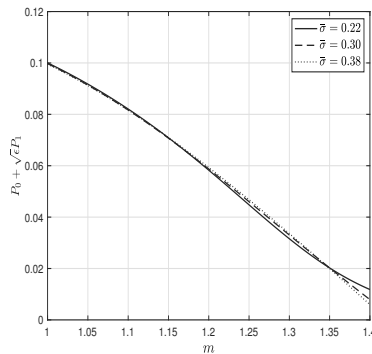
(c) Option value of the option with respect to time-to-maturity with $\bar{\sigma} = 0.22, 0.30, 0.38$

FIGURE 4. Option values of P_0 , P_1 and $P_0 + \sqrt{\epsilon}P_1$ with respect to effective volatility ($r = 0.040, q = 0.045, m = 1.1, \epsilon = 0.007$ and $s/m = 0.9$).

the Monte Carlo simulation and the analytically approximated solution are implemented by utilizing an Intel i7-6700 CPU (3.40 GHz, 16 GB RAM). As seen in Tables 2 and 3, as ϵ increases or the number of simulations increases, the numerical solution from the Monte Carlo simulation, which is regarded as a good approximation in a real-world solution, gets closer to our analytic solution. This finding means that the approximated formula presented in (32) provides an accurate solution for the American lookback options.



(a) Option value of the leading-order term with respect to maximum process $\bar{\sigma} = 0.22, 0.30, 0.38$
 (b) Option value of the correction term with respect to maximum process $\bar{\sigma} = 0.22, 0.30, 0.38$



(c) Option value of the option with respect to maximum process $\bar{\sigma} = 0.22, 0.30, 0.38$

FIGURE 5. Option values of P_0 , P_1 and $P_0 + \sqrt{\epsilon}P_1$ with respect to effective volatility ($r = 0.040, q = 0.045, \epsilon = 0.007$ and $\tau = 0.02$).

6. Concluding remarks

In this study, we investigate the approximated solutions of the American lookback options and their optimal exercise boundaries under a SV model introduced by Fouque et al. [17], which accounts for the nature of SVs in the financial market. First, we find the PDEs for the value of the American lookback options using the underlying asset models, and by exploiting a singular perturbation method and the LCTs, we obtain analytic formulas for the corrected option value. For inverting the LCTs, we use the Gaver-Stehfest methods

TABLE 2. The change in the price difference between the Monte-Carlo price P_{MC} and the corrected solution \bar{P} with respect to the ϵ . Note that (i) the # of simulations for the Monte Carlo simulation is 10,000, (ii) CI means confidence interval, and (iii) $RE = \frac{|P_{MC} - \bar{P}|}{P_{MC}} \times 100$. Selected parameters are $m = 1.55, \nu = 0.5, q = 0, r = 0.02, \rho = 0.1, S_0 = 1, Y_0 = 0, \bar{\sigma} = 0.22, T = 1, \theta = 0, \Lambda(y) = 0, f(y) = e^y, V_2 = 0.0188$, and $V_3 = 0.0094$.

ϵ	P_{MC}	CI (95%)	\bar{P}	$ P_{MC} - \bar{P} $	RE (%)
10^{-3}	0.505517	[0.192431,0.818604]	0.561292	0.055774	11.033122
10^{-4}	0.537304	[0.507823,0.566785]	0.550957	0.013653	2.540986
10^{-5}	0.555665	[0.540580,0.570750]	0.547689	0.007976	1.435441
10^{-6}	0.542206	[0.528808,0.555604]	0.546655	0.004449	0.820595

TABLE 3. The change in the price difference between the Monte-Carlo price P_{MC} and the corrected solution \bar{P} with respect to # of simulations for Monte-Carlo method ($\epsilon = 10^{-6}$). Note that (i) CI means confidence interval, (ii) $RE_1 = \frac{|P_{MC} - P_0|}{P_{MC}} \times 100$, and (iii) $RE_2 = \frac{|P_{MC} - \bar{P}|}{P_{MC}} \times 100$. The parameters are given by $m = 1.55, \nu = 0.5, q = 0, r = 0.02, \rho = 0.1, S_0 = 1, Y_0 = 0, \bar{\sigma} = 0.22, T = 1, \theta = 0, \Lambda(y) = 0, f(y) = e^y, V_2 = 0.0188$, and $V_3 = 0.0094$.

# of paths	P_{MC}	CI (95%)	P_0	$\bar{P} (\epsilon = 10^{-6})$	$ P_{MC} - P_0 $	RE ₁ (%)	$ P_{MC} - \bar{P} $	RE ₂ (%)
10,000	0.542 206	[0.528 808,0.555 604]	0.550 405	0.546 655	0.008 199	1.512 189	0.004 449	0.820 595
20,000	0.548 140	[0.541 056,0.555 225]	0.550 405	0.546 655	0.002 265	0.413 182	0.001 485	0.270 925
30,000	0.547 043	[0.538 210,0.555 875]	0.550 405	0.546 655	0.003 362	0.614 634	0.000 388	0.070 846
50,000	0.546 888	[0.541 774,0.552 002]	0.550 405	0.546 655	0.003 517	0.643 085	0.000 233	0.042 588
100,000	0.546 590	[0.543 066,0.550 113]	0.550 405	0.546 655	0.003 816	0.698 057	0.000 066	0.012 010

stated in Appendix B in detail. Second, based on the analytical solutions, we verify that our first-approximated solution comes up with an accurate formula of the American lookback options compared with the Monte Carlo price. Third, from the numerical experiments, we investigate the quantitative and qualitative influence of our approximated solutions by analyzing the fast mean-reverting process contained in the SV model. We can notice that the impact of the SV on the movements of the option prices and the free-boundary values in the American lookback options is very sensitive to time-to-maturity, effective volatility

or the maximum process. Finally, many researchers are currently working on the American options or exotic options using the LCTs for higher-dimensional model dynamics in financial mathematics. For further research, our chosen American lookback option could be extended to a more complicated American option with other types.

Appendix A. Basic properties of the Laplace-Crson transforms

Referring to [25], we can derive some useful properties from the definition of the LCTs.

$$\begin{aligned}\mathcal{LC}\left[\frac{d}{dx}\chi(x)\right](\lambda) &= \lambda(\chi^*(\lambda) - \chi(0+)), \\ \mathcal{LC}\left[\chi^{(n)}(x)\right](\lambda) &= \lambda^n\chi^*(\lambda) - \sum_{k=0}^{n-1}\lambda^{n-k}\chi^{(k)}(0+) \quad \text{for } n = 1, 2, \dots, \\ \mathcal{LC}\left[\int_0^x\chi(y)dy\right](\lambda) &= \frac{1}{\lambda}\chi^*(\lambda), \\ \mathcal{LC}\left[\frac{\chi(x)}{x}\right](\lambda) &= \lambda\int_\lambda^\infty\frac{\chi^*(s)}{s}ds, \\ \mathcal{LC}[\chi(x-a)1_{\{x\geq a\}}(x)](\lambda) &= e^{-a\lambda}\chi^*(\lambda), \quad a > 0, \\ \mathcal{LC}[e^{ax}\chi(x)](\lambda) &= \frac{\lambda}{\lambda-a}\chi^*(\lambda-a), \\ \mathcal{LC}\left[\chi\left(\frac{x}{a}\right)\right](\lambda) &= \chi^*(a\lambda), \quad a > 0.\end{aligned}$$

Appendix B. The review of the Gaver-Stehfest methods

In this appendix, we introduce the method of the Laplace-Carson inverse transforms. This inverse algorithm is applied to the results obtained from Theorem 4.1 and Theorem 4.2 in Section 4. There are several methods used for Laplace-Carson inverse transformation, such as the post-width, Laguerre, and Gaver-Stehfest methods. Because it is convenient for us to deal with the Gaver-Stehfest method (Gaver [18]; Stehfest [31]) and it is less robust than other methods (cf. Kimura [24]), we used the method for numerical experiments. A detailed description of this method is presented in [1], and the sufficient condition for the integrand function ψ for the LCTs, where the convergence of ψ is guaranteed as the limit of an extrapolation function ψ_n , is described in [27].

Referring to Kimura [24], let us consider the LCT $\hat{\psi}$ of a locally integrable function $\psi : (0, \infty) \rightarrow \mathbb{R}$

$$\hat{\psi}(\lambda) := \int_0^\infty \lambda e^{-\lambda\tau} \psi(\tau) d\tau,$$

where the integrand function ψ is approximately expressed by $\psi_n(\tau)$, and $\psi_n(\tau) := \psi_n^{(n)}(\tau)$ ($n \geq 1$) is generated by the recursive sequence $\{\psi_n^{(m)} : n, m = 1, 2, \dots\}$ such that

$$\begin{aligned}\psi_0^{(m)}(\tau) &:= \hat{\psi}\left(m \frac{\log 2}{\tau}\right), \\ \psi_n^{(m)}(\tau) &:= \left(1 + \frac{m}{n}\right) \psi_{n-1}^{(m)}(\tau) - \frac{m}{n} \psi_{n-1}^{(m+1)}(\tau), \quad n = 1, 2, \dots\end{aligned}$$

However, because the method has a disadvantage in that the speed of convergence is slow, Stehfest [31] suggested an auxiliary extrapolation function

$$(33) \quad \psi_n^*(\tau) = \sum_{k=1}^n \frac{(-1)^{n-k} k^n}{k!(n-k)!} \psi_k(\tau)$$

to improve the calculation speed. In other words, $\{\psi_n^*(\tau) : n = 1, 2, \dots\}$ converges to ψ faster than $\{\psi_n(\tau) : n = 1, 2, \dots\}$, as mentioned by Kimura [24]. Thus, Equation (33) is said to be the n -th extrapolation **Gaver-Stehfest methods**. According to Stehfest [31], ψ_n^* converges to ψ sufficiently in the case of $n \geq 4$, and the relative errors of the approximation are less than 10^{-4} . In this study, we used the Gaver-Stehfest method with the 5-th extrapolation for pricing accuracy.

References

- [1] J. Abate and W. Whitt, *A unified framework for numerically inverting Laplace transforms*, INFORMS J. Comput. **18** (2006), no. 4, 408–421. <https://doi.org/10.1287/ijoc.1050.0137>
- [2] A. Agarwal, S. Juneja, and R. Sircar, *American options under stochastic volatility: control variates, maturity randomization & multiscale asymptotics*, Quant. Finance **16** (2016), no. 1, 17–30. <https://doi.org/10.1080/14697688.2015.1068443>
- [3] F. Black and M. Scholes, *The pricing of options and corporate liabilities*, J. Polit. Econ. **81** (1973), no. 3, 637–654. <https://doi.org/10.1086/260062>
- [4] P. Carr, *Randomization and the American put*, Rev. Financ. Stud. **11** (1998), no. 3, 597–626.
- [5] S.-Y. Choi, J.-P. Fouque, and J.-H. Kim, *Option pricing under hybrid stochastic and local volatility*, Quant. Finance **13** (2013), no. 8, 1157–1165. <https://doi.org/10.1080/14697688.2013.780209>
- [6] S.-Y. Choi, V. Sotheara, J.-H. Kim, and J.-H. Yoon, *A Mellin transform approach to the pricing of options with default risk*, Comput. Economics (2021), Online published.
- [7] S.-Y. Choi, J.-H. Yoon, and J. Jeon, *Pricing of fixed-strike lookback options on assets with default risk*, Math. Probl. Eng. **2019** (2019), Art. ID 8412698, 10 pp. <https://doi.org/10.1155/2019/8412698>
- [8] A. Conze and R. Viswanathan, *Path dependent options: The case of lookback options*, J. Finance **46** (1991), no. 5, 1893–1907.
- [9] M. Dai, *A closed form solution to perpetual American floating strike lookback option*, J. Comput. Finance **4** (2000), no. 2, 63–68.
- [10] M. Dai and Y. K. Kwok, *American options with lookback payoff*, SIAM J. Appl. Math. **66** (2005), no. 1, 206–227. <https://doi.org/10.1137/S0036139903437345>

- [11] M. Dai and Y. K. Kwok, *Characterization of optimal stopping regions of American Asian and lookback options*, Math. Finance **16** (2006), no. 1, 63–82. <https://doi.org/10.1111/j.1467-9965.2006.00261.x>
- [12] M. Dai, H. Y. Wong, and Y. K. Kwok, *Quanto lookback options*, Math. Finance **14** (2004), no. 3, 445–467. <https://doi.org/10.1111/j.0960-1627.2004.00199.x>
- [13] J.-P. Fouque, G. Papanicolaou, and R. Sircar, *Financial modelling in a fast mean-reverting stochastic volatility environment*, Asia-Pacific Financial Markets **6** (1999), no. 1, 37–49.
- [14] J.-P. Fouque, G. Papanicolaou, and R. Sircar, *Mean-reverting stochastic volatility*, Intern. J. Theor. Appl. Finance **3** (2000), no. 1, 101–142.
- [15] J.-P. Fouque, G. Papanicolaou, and K. R. Sircar, *From the implied volatility skew to a robust correction to Black-Scholes American option prices*, Int. J. Theor. Appl. Finance **4** (2001), no. 4, 651–675. <https://doi.org/10.1142/S0219024901001139>
- [16] J.-P. Fouque, G. Papanicolaou, R. Sircar, and K. Solna, *Singular perturbations in option pricing*, SIAM J. Appl. Math. **63** (2003), no. 5, 1648–1665. <https://doi.org/10.1137/S0036139902401550>
- [17] J.-P. Fouque, G. Papanicolaou, R. Sircar, and K. Solna, *Multiscale stochastic volatility for equity, interest rate, and credit derivatives*, Cambridge University Press, Cambridge, 2011. <https://doi.org/10.1017/CB09781139020534>
- [18] D. P. Gaver, Jr., *Observing stochastic processes, and approximate transform inversion*, Operations Res. **14** (1966), 444–459. <https://doi.org/10.1287/opre.14.3.444>
- [19] M. B. Goldman, H. B. Sossin, and M. A. Gatto, *Path dependent options: Buy at the low, sell at the high*, J. Finance **34** (1979), no. 5, 1111–1127.
- [20] S. L. Heston, *A closed-form solution for options with stochastic volatility with applications to bond and currency options*, Rev. Financ. Stud. **6** (1993), no. 2, 327–343. <https://doi.org/10.1093/rfs/6.2.327>
- [21] M. Kang, J. Jeon, H. Han, and S. Lee, *Analytic solution for American strangle options using Laplace-Carson transforms*, Commun. Nonlinear Sci. Numer. Simul. **47** (2017), 292–307. <https://doi.org/10.1016/j.cnsns.2016.11.024>
- [22] I. Karatzas and S. E. Shreve, *Brownian motion and stochastic calculus*, second edition, Graduate Texts in Mathematics, 113, Springer-Verlag, New York, 1991. <https://doi.org/10.1007/978-1-4612-0949-2>
- [23] T. Kimura, *Valuing finite-lived Russian options*, European J. Oper. Res. **189** (2008), no. 2, 363–374. <https://doi.org/10.1016/j.ejor.2007.05.026>
- [24] T. Kimura, *American fractional lookback options: valuation and premium decomposition*, SIAM J. Appl. Math. **71** (2011), no. 2, 517–539. <https://doi.org/10.1137/090771831>
- [25] T. Kimura, *Applications of the Laplace-Carson transform to option pricing: A tutorial*, Kyoto University Research Information Repository **1983** (2016), 68–89.
- [26] T. Kimura, *A refined Laplace-Carson transform approach to valuing convertible bonds*, J. Oper. Res. Soc. Japan **60** (2017), no. 2, 50–65. <https://doi.org/10.15807/jorsj.60.50>
- [27] A. Kuznetsov, *On the convergence of the Gaver-Stehfest algorithm*, SIAM J. Numer. Anal. **51** (2013), no. 6, 2984–2998. <https://doi.org/10.1137/13091974X>
- [28] M.-K. Lee, *Pricing perpetual American lookback options under stochastic volatility*, Comput. Econ. **53** (2019), 1265–1277.
- [29] K. S. Leung, *An analytic pricing formula for lookback options under stochastic volatility*, Appl. Math. Lett. **26** (2013), no. 1, 145–149. <https://doi.org/10.1016/j.aml.2012.07.008>
- [30] A. G. Ramm, *A simple proof of the Fredholm alternative and a characterization of the Fredholm operators*, Amer. Math. Monthly **108** (2001), no. 9, 855–860. <https://doi.org/10.2307/2695558>

- [31] H. Stehfest, *Algorithm 368: Numerical inversion of Laplace transforms*, Communications of the ACM **13** (1970), 47–49.
- [32] L. N. Tao, The analyticity and general solution of the Cauchy-Stefan problem, Quart. J. Mech. Appl. Math. **36** (1983), no. 4, 487–504. <https://doi.org/10.1093/qjmam/36.4.487>
- [33] H. Y. Wong and C. M. Chan, *Lookback options and dynamic fund protection under multiscale stochastic volatility*, Insurance Math. Econom. **40** (2007), no. 3, 357–385. <https://doi.org/10.1016/j.insmatheco.2006.05.006>
- [34] H. Y. Wong and Y. K. Kwok, *Sub-replication and replenishing premium: Efficient pricing of multi-state lookbacks*, Rev. Deriv. Res. **6** (2003), no. 2, 83–106.
- [35] H. Y. Wong and J. Zhao, *Valuing American options under the CEV model by Laplace-Carson transforms*, Oper. Res. Lett. **38** (2010), no. 5, 474–481. <https://doi.org/10.1016/j.orl.2010.07.006>
- [36] Z. Zhou and H. Wu, *Laplace transform method for pricing American CEV strangles option with two free boundaries*, Discrete Dyn. Nat. Soc. **2018**, Art. ID 5908646, 12 pp. <https://doi.org/10.1155/2018/5908646>
- [37] S.-P. Zhu and W.-T. Chen, *Pricing perpetual American options under a stochastic-volatility model with fast mean reversion*, Appl. Math. Lett. **24** (2011), no. 10, 1663–1669. <https://doi.org/10.1016/j.aml.2011.04.011>

DONGHYUN KIM
DEPARTMENT OF MATHEMATICS
PUSAN NATIONAL UNIVERSITY
BUSAN 46241, KOREA
Email address: donghyunkim@pusan.ac.kr

JUNHUI WOO
DEPARTMENT OF MATHEMATICS
PUSAN NATIONAL UNIVERSITY
BUSAN 46241, KOREA
Email address: woowoowo47@gmail.com

JI-HUN YOON
DEPARTMENT OF MATHEMATICS
PUSAN NATIONAL UNIVERSITY
BUSAN 46241, KOREA
Email address: yssci99@pusan.ac.kr